

Re-Cellularised Kidney Scaffold for Chikungunya Virus Propagation: A Novel Approach

Sonal Walawalkar¹ · Shahdab Almelkar¹ 

Received: 20 December 2021 / Revised: 12 February 2022 / Accepted: 3 March 2022 / Published online: 9 May 2022
© Korean Tissue Engineering and Regenerative Medicine Society 2022

Abstract

BACKGROUND: Re-emerging viral attacks are catastrophic for health and economy. It is crucial to grasp the viral life cycle, replication and mutation policies and attack strategies. It is also absolute to fathom the cost-efficient antiviral remedies earliest possible.

METHODS: We propose to use a lab-grown organ (re-cellularized scaffold of sheep kidney) for viral culture and understand its interaction with extra-cellular matrices of the host tissue.

RESULTS: Our findings showed that the chikungunya virus (CHIKV) could be better replicated in tissue-engineered bio models than cell culture. A decrease in ds-DNA levels emphasized that CHIKV propagates within the re-cellularized and cell culture models. There was an increase in the viral titres (pfu/ml) in re-cellularized scaffolds and control groups. The lipid peroxidation levels were increased as the infection was progressed in cell culture as well as re-cellularized and control groups. The onset and progress of the CHIKV attacks (cellular infection) lead to transmembrane domain fatty acid peroxidation and DNA breakdown, landing in cellular apoptosis. Simultaneously cell viability was inversely proportional to non-viability, and it decreased as the infection progressed in all infected groups. Histological findings and extracellular matrix evaluation showed the impairment in medullary, cortex regions due to propagation of CHIKV and plaques generations.

CONCLUSION: This method will be a breakthrough for future virus culture, drug interaction and to study its effect on extracellular matrix alterations. This study will also allow us to investigate the correct role of any vaccine or antiviral drugs and their effects on re-engineered organ matrices before moving towards the animal models.

Keywords Re-cellularization · Chikungunya virus culture · Plaque assay · Lipid peroxidation · Histology · Bio-model

1 Introduction

The knowledge of the viral life cycle and its propagation is crucial for establishing a protocol to combat the virus, making appropriate antiviral drugs and vaccines. Abundant

viral titre is essential in such research areas. Traditional methods of viral cultures are not without drawbacks. Here, we present a unique combination of tissue-engineered organs for viral growth and compare it with viral growth using both culture media and the whole organ.

Chikungunya virus (CHIKV) is a mosquito-transmitted re-emerging alphavirus capable of an epidemic with periodic and explosive outbreaks [1]. Severe debilitating polyarthritides and myalgia can persist for years of post-infection, affecting over 1 million globally [2, 3]. Despite such catastrophes, we are still at a loss of understanding its life cycle, mode of attack, and combating remedies.

✉ Shahdab Almelkar
healthbiolabs@gmail.com

¹ HEALTH BIOLABS Pvt. Ltd., Division of Tissue Engineering and Cell Science (TECS), Shree Hospital and Research Institute (SHRI), 1st Lane Rajarampuri, Kolhapur, Maharashtra 416008, India

Currently, CHIKV is handled and propagated in Vero cell lines (monkey kidney origin). Surprisingly, its target organs are cartilage, bones, and joints without any renal impairment. After entering Vero cells by clathrin-mediated endocytosis (CME), its effect on cellular and extracellular matrix (ECM) is unknown [4]. Further, a particular question needs to be addressed: Does CHIKV infects kidney cells primarily and form a small reservoir for its propagation (plaques generations) followed by CHIKV migration to the target tissues? During CHIKV infection and propagation, does it cause any alteration cellular or extracellular matrix? Also, does it develop any acute or chronic renal or nephrological pathology?

Furthermore, even if vaccination is the most promising means to protect people in regions with endemic CHIKV, challenging balance between vaccine safety, immunogenicity, and economic production constraints impedes CHIKV vaccine development and license [4, 5]. Thus, treatment is limited to only palliative care [4, 5]. It is vital to get an abundant, faster, and economic CHIKV population to answer all problems.

Recently, the esteemed technology of decellularization followed by re-cellularization has made a mark in organ engineering [6, 7]. We utilized this technology for CHIKV growth. We remodelled the sheep kidney by decellularization (SKD) and followed by re-cellularization (using Renal and Vero cells). Further, we propagated CHIKV into this bio-model to study its titre and understand its pathology in Renal and Vero cells and its interaction with ECM. We compared viral propagation in whole sheep kidney, Renal and Vero cell lines in culture by plaque assays. Our study also highlight the onset of inflammatory response (enhanced malondialdehyde levels) in the CHIKV-infected cells. This study establishes a new frontier in virology and bio-engineering (regenerative medicine), which will be a stepping stone towards changing research angles in the field of vaccine or antiviral drug testing with the possibilities of avoiding non-clinical (animal) trials.

2 Materials and methods

2.1 Grouping

The grouping was done as per Table 1.

2.2 Dissection, cannulation and perfusion

SKDs were rinsed in sterile PBS 1X containing antibiotics (ciprofloxacin 100 IU/L,) after removing adrenal glands and fat tissues. Renal artery was identified, cannulated, and perfused with 1000 ml normal saline and RBC lysis buffer, ionic 1% SDS (HIMEDIA, Mumbai, India) under gravity's

influence (Group II, n = 5). The procedure was carried till SKDs became completely translucent [8].

2.3 Histology and ECM evaluation

Perfused (Group II) and non-perfused kidneys (Group I) were fixed in 10% formaldehyde solution (Himedia), processed for paraffin wax embedded blocks, and trimmed onto sections of 5 microns on a rotary microtome. Hematoxylin and eosin (H&E) staining was done for histology. Verhoff von-Gieson staining (Qualigens, Mumbai, India) was done for ECM evaluation.

2.4 DNA quantification

All samples in Groups I, II, III, IV, V, IA, IIA, IIIA, IVA, VA were placed in lysis buffer for 20 min, crushed and centrifuged. Genomic DNA Isolation Kit, NORGEN BIOTEK CORPORATION, Thorold, ON, Canada, was used for DNA isolation. Eluted ds-DNA levels were quantified by (Picogreen) fluorescent assay at 260–280 nm on UV-Visible spectrophotometer [Biotechk, Synergy (SLFX)] for presence or absence of residual ds-DNA.

2.5 Renal cell isolation and culture

SKD was minced, incubated in Collagenase type I (0.2%, Sigma, USA) at 37 °C for 45 min, and centrifuged at 2000 rpm. Isolated cells were suspended in Dulbecco's modified eagle medium (DMEM) (GIBCO-BRL, Grand Island, NY, USA) containing 20% fetal bovine serum (GIBCO-BRL), 2% L-glutamine, leukemia inhibitory factor (0.2 µg/ml), penicillin and streptomycin (2.0%) (GIBCO-BRL). Cells were seeded onto T-25 culture flasks at a density of 0.1 million (1.0×10^5) cells/ml and incubated in a CO₂ incubator at 37 °C with 5% CO₂ (Group III). The medium was changed every 24 h. Cells were maintained till a confluence of 80%, which was attained in about 21 days. Then cells were dislodged using 0.5 ml 0.025% collagenase type I (Sigma-Aldrich, St. Louis, MO, USA) solution. They were maintained till five subcultures.

2.6 Vero cell culture

Vero cells (Monkey origin) were cultured (Group IV, n = 5) using DMEM (Himedia). They were supplemented with 5% Fetal Bovine Serum (FBS, Gibco, Grand Island, NY, USA), anti-mycotic and antibiotic solution (Sigma).

2.7 CHIKV-infected serum

Patient serum was obtained and tested for CHIKV nsp-1 protein on an Advantage Chikungunya Card rapid kit (Lot

Table 1 DNA quantification, LPO levels, plaque assays, MTT assays

Groups mean \pm SD)	DNA (Mean ng/ ml \pm SD)	LPO (Mean nmoles /ml/ mg protein \pm SD)	Plaque assay [Mean transformed value] [pfu/ml \pm SD]	Cell viability (% Mean \pm SD)	Non-viability (% Mean \pm SD)
I (n = 5)	6368 ng/ml \pm 200.6	36.30 \pm 6.792	–	95.49% \pm 3.264	4.51% \pm 3.264
II (n = 5)	12.97 ng/ml \pm 3.453	0.4222 \pm 0.342	–	–	–
III (n = 5)	1979 ng/ml \pm 103	7.08 \pm 3.248	–	65.36% \pm 4.896	34.64% \pm 4.896
IV (n = 5)	4854 ng/ml \pm 300	6.320 \pm 2.179	–	70.14% \pm 4.161	29.86% \pm 4.161
V (n = 5)	5482 ng/ml \pm 324.1	17.92 \pm 3.937	–	77.76% \pm 5.698	22.24% \pm 5.698
IA (n = 5)	2724 ng/ml \pm 558.2	57.40 \pm 4.118	5.960 \pm 0.02	48.34% \pm 5.160	51.66% \pm 5.160
IIA (n = 5)	2.033 ng/ml \pm 2.050	0.4140 \pm 0.283	–	–	–
III A (n = 5)	1073 ng/ml \pm 18.82	26.94 \pm 2.177	105.925 \pm 0.054	32.86% \pm 4.888	67.14% \pm 4.888
IV A (n = 5)	1137 ng/ml \pm 39.95	17.22 \pm 2.148	106.285 \pm 0.033	26.92% \pm 4.462	73.28% \pm 4.361
V A (n = 5)	556.0 ng/ml \pm 157.1	38.78 \pm 3.011	6.282 \pm 0.023	17.28% \pm 1.539	82.72% \pm 1.539

**Group I: sheep kidney (SK), Group II: decellularized SKD, Group III: Renal cell culture, Group IV: Vero cell culture, Group V: Perfusion of kidney + renal cells + vero cells, Group IA: non-decellularized control kidney + CHIKV infection, Group IIA: Decellularized + CHIKV, Group IIIA: Renal cells + CHIKV infection, Group IVA: Vero cells + CHIKV infection, Group VA: Perfusion of renal cells + Vero cells + CHIKV infection

Number; CMC041220, J. Mitra & Co. Pvt. Ltd, India). The rapid diagnostic test was done for quantitative detection of CHIKV nsp-1 protein-positive serum which was used for further studies.

2.8 CHIKV infection and culture

1 ml serum was diluted in 9 ml of MEM high glucose cell culture medium (1:10). Diluted MEM was overlaid onto confluent Vero cells in a T-75 flask (Group IV A). After 48 h cytopathological effect (CPE) was observed, and virus titre was obtained with serial dilutions.

2.9 Immunocytochemistry

Approximately 5×10^4 Vero E6 cells were seeded in a six-well plate with coverslips. Cells were allowed to form a confluent monolayer on coverslips, infected with CHIKV, and incubated for 12 h. Later, they were fixed by chilled acetone and methanol in a 1:1 ratio for 15–20 min. Coverslips were washed with PBS and 0.1% Tween-20 (PBST) thrice, blocked with 1% bovine serum albumin (BSA) (Sigma-Aldrich) in PBS, and incubated for 1 h at room temperature (RT). Further, they were incubated with (1:200) mouse anti-CHIKV antibody followed by incubation with FITC-conjugated rabbit anti-mouse (1:400) antibodies (Invitrogen, Carlsbad, CA, USA). Slides were visualized using a fluorescence microscope (Nikon eclipse T2000S and Q capture pro 5.0 software, Tokyo, Japan). Negative controls were similarly processed using pre-immune sera.

2.10 Cells infection with CHIKV and plaque assay

Cultured renal cells were expanded and infected with 0.01 MOI (CHIKV). After 48 h, CPE was observed, and cells (Group III A) were allowed to burst at a lower temperature – 70 °C for virus release into suspensions soup. The suspension was centrifuged, cellular debris was discarded, and the supernatant was used for plaque assay. Vero E9 cell line was used for plaque assay studies. Vero E9 cells (100,000 cells/well) were plated in every single well of the culture plate. Cells were incubated for 24 h till they achieved confluence. Virus suspension (0.01 MOI) was used for plaque assay, and viral titres (1:10 serial dilutions) were obtained. Vero cells were refreshed with PBS 1X and overlaid with 2% carboxymethyl cellulose (CMC) in 2X DMEM (high glucose) with 1% FBS (Thermo Fisher Scientific, Waltham, MA, USA). Plate was incubated for 48 h at 37 °C with 5% CO₂. Plate was then stained with 0.1% crystal violet in formal saline. Plaques were counted and expressed as plaque-forming units per ml (pfu/mL).

2.11 Re-cellularisation of the scaffold, virus infection, and plaque assays

Cultured renal and Vero cells (approximately 1 million cells each) expanded in culture were trypsinized and perfused into decellularized kidney scaffold through the renal artery. Other ends of the renal vein and ureter were clamped. Further, 1 ml of 2% FBS containing DMEM (Himedia, India) was perfused, and the entire kidney scaffold was incubated in a CO₂ incubator for 78 h. After 8 h, clamped ends were opened, and the medium was

allowed to drain. Again DMEM perfusion for 8 h was done with re-clamping for perfused renal and vero cells to remodel in the entire glomerular network. Cellular feeding was carried for 21 days. After 21 days, perfusion of CHIKV (0.01 MOI) was carried out to infect re-cellularized kidney scaffolds. Simultaneously, the control kidney was infected with CHIKV with 0.01 MOI. The virus was allowed to infect and propagated in the kidney (control) for 24 h till we found gross pathological infection or plaque-like generation. Finally, the virus-containing soup was drained from kidney scaffolds and control the kidney, and headed for plaque assay in the vero cell line to assess viral titres and infectivity.

2.12 Trypan blue and crystal violet dye injection

Group II kidney capsule was injected with 0.01% Trypan blue (HIMEDIA) to localize kidney scaffold architecture (Group II). Group IA, Group VA were perfused with 1% crystal violet to assess white translucent patches (plaques) for demarcating CHIKV propagation.

2.13 Malondialdehyde

Lipid peroxidation (malondialdehyde) levels were quantified for Groups I, II, III, IV, V, IA, IIA, IIIA, IVA, VA. LPO-BIOXY 586 kit, (BIOXY, GmbH) was used to quantify lipid peroxidation levels. All experimental sets were macerated in lysis buffer and chilled Tris buffer (20 mM, pH 7.4). About 200 µl of cellular soups were taken for the reaction. Approximately, 650 µl R1 reagents (N-methyl-2-phenylindole) were added and 100 µl of 1 N HCL were added (reaction mixture). All cocktail mixture was incubated for 1 h at 80 °C till pink color was developed. Further, absorbance was taken at 530 nm for MDA measurement.

2.14 MTT assays

Cell viability and non-viability were assessed by MTT assay. CHIKV suspension was obtained from Group I, Group III, Group IV, Group V, Group I A, Group III-A, Group IV A, Group VA. 0.01 MOI was maintained for infection to cells (perfused and non-perfused, cultured). Group I, Group IA, Group V, Group VA, the MTT assay solution (5 mg/ml) (HIMEDIA) was perfused, and incubation was carried for 3 h. Group III, Group IV, Group IIIA and Group IV A MTT (5 mg/ml) solution was added to cultured wells, and incubation was carried for 3 h in a CO₂ incubator. Dark blue color formazon crystals formed in perfused and directly added MTT solutions were dissolved in 1 ml of DMSO solution, and absorbance was taken on 520–630 nm.

2.15 Statistics

GraphPad Prism 5 software was used to obtain the mean ± standard deviation, and a one-way ANOVA (***) $p < 0.0001$ test was performed, and the graph was obtained.

3 Results

3.1 Kidney decellularization by perfusion

Perfusions of solvents showed progressive morphological changes in texture (Fig. 1A). Change in color from dark red to grey to translucent was seen in 6 days (Fig. 1). Mosaic patches (14 h) in the medullary region with translucent renal microvasculature appeared after 12 h (Fig. 1C).

3.2 Histology

Histology for Group I (Fig. 2) showed normal renal cellular and ECM (Fig. 2A). EVG staining showed intact elastin and collagen in dark red color. No abnormality was seen in Group I ECM (Fig. 2C). H–E staining revealed the absence of cuboidal, columnar epithelial cells in the cortex (glomerulus knot, BC, PCT) and medulla zones for Group II (Fig. 2B), while loop of Henle was difficult to appreciate. DCT, with its opening in CT, could be seen in the medulla. Stroma without mesangial cells was appreciated in between PCT and DCT regions (Fig. 2C). No abnormality of ECM was observed after decellularization (Fig. 2C). Glomerulus shows ghost outline for Group II scaffolds, and EVG staining showed fragmentation in elastic lamina and micro-vessel (Fig. 2D).

3.3 DNA quantification

A decrease in ds-DNA was observed in Group I and IA (3664 ng/ml), Group III and Group IIIA (906 ng/ml), Group IV and Group IVA (3681 ng/ml), Group V and Group VA (4926 ng/ml). The ds-DNA was lesser for CHIKV infection groups than non-infected groups (Fig. 3) (Table 1).

3.4 Renal and vero cell culture

Renal cells were maintained till five sub-cultures. First primary isolation had reached confluency after 21 days (Fig. 4). Renal cells showed spindle shape in culture during an expansion (Fig. 4A). Further, they formed a Whirlpooling pattern with expanded pseudopodia. As sub-culture progressed, they altered their phenotype to a more

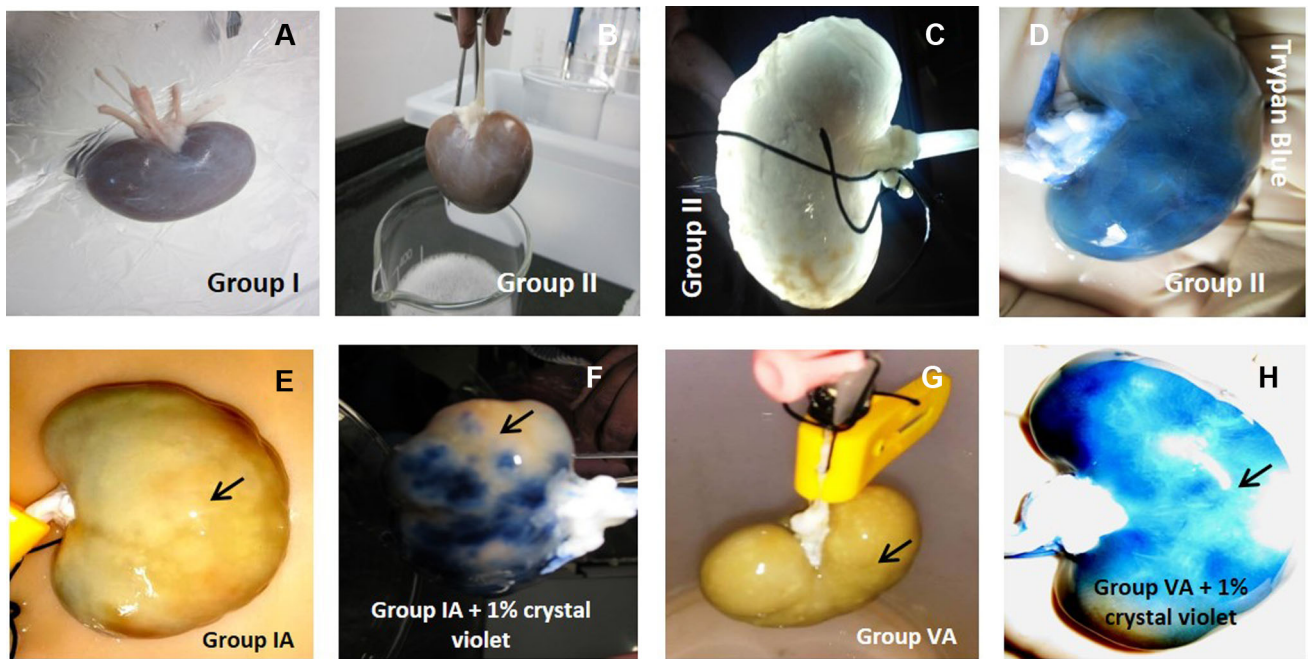
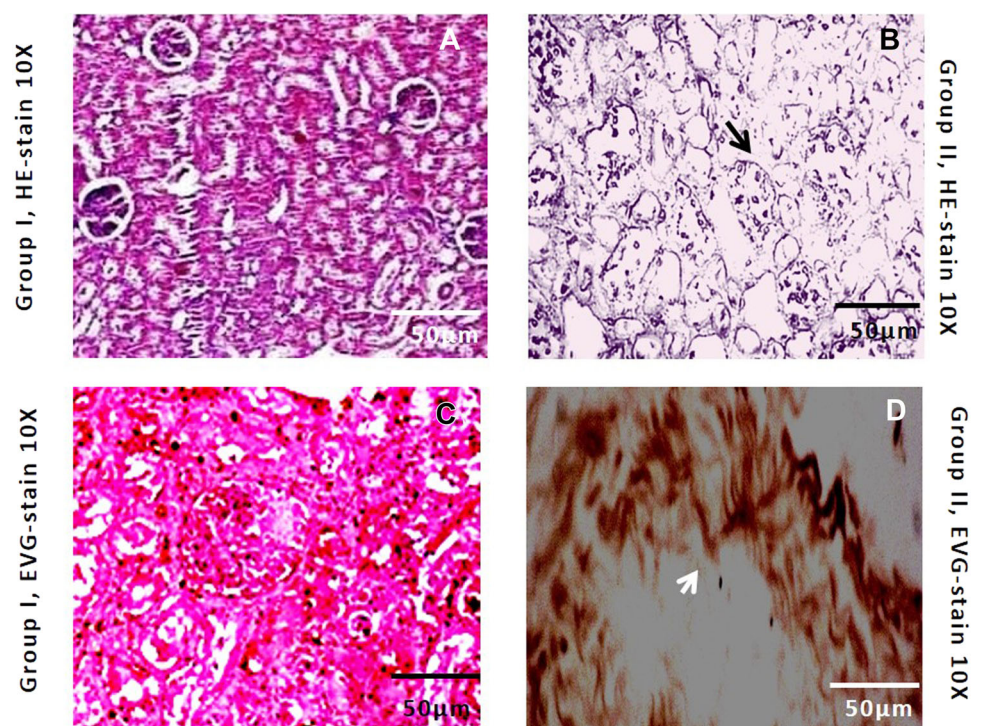


Fig. 1 The process of decellularization by lagendroff method and re-cellularization as well as CHIKV infection. **A** The Group I non-processed and dissected kidney with clear renal artery, vein, and ureter is seen. **B** The suspended kidney and 1% SDS perfusion are seen during the process of decellularization. **C** Group II completely decellularised ghost kidney with intact cortex and renal capsule. **D** The nephrological micro-vasculature (Group II), including glomeruli networks, is observed through 0.01% trypan blue dye perfusion. **E** CHIKV perfused (Group IA) and infected (arrow) in the

non-decellularised sheep kidney showing virological pathology (plaque lesions) in cortex (arrow) and medulla. **F** 1% crystal violet dye perfused through Group IA kidney scaffold showing plaques generation (translucent Zones) indicating CHIKV replication (arrow). **G** Re-cellularized and CHIKV-infected (Group VA) showing more or less similar virological pathology (arrow) like Group IA. **H** Group VA shows larger gross plaques (arrows) with the occurrence of translucent patches and fused zone indicating the CHIKV replications (plaque colonies) within the kidney scaffold capsule

Fig. 2 **A** Group I (Hematoxylin and Eosin) staining showed the clear cytological appearance of Bowman’s capsule, PCT, and DCT with clear presence of cuboidal cells. **B** Group II showed the absence of any cells leaving behind only glomeruli scaffolds (arrows). **C** The Verhoff von-Gieson (EVG) stain clearly showed the presence of collagen and elastin matrix in the glomeruli zones. **D** The EVG stain is positive for Group II kidney scaffold with elastic (arrow) matrices and occurrence of collagen substances



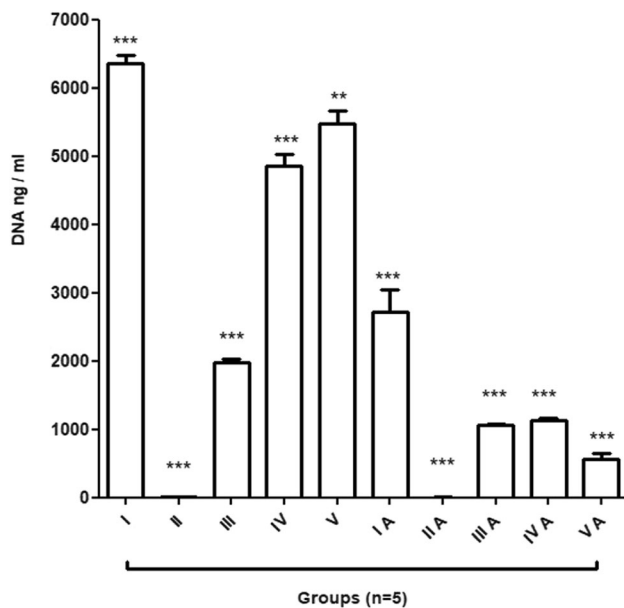


Fig. 3 DNA quantification (Picogreen) analysis for the infected and non-infected groups. Group I showed higher DNA ng/ml than all other groups with one-way analysis of variance (Tukey's test) $***p < 0.0001$. Picogreen DNA ng/ml analysis showing a complete absence of host cellular genetic material for Group II ($n = 5$) and Group IIA ($n = 5$), showing a one-way ANOVA $***p < 0.0001$ level of significance. Groups III ($n = 5$) and IV ($n = 5$) showed stepwise rise DNA ng/ml and One-way ANOVA $***p < 0.0001$. However, Group IIIA and Group IVA showed a reduction in DNA ng/ml than Group III and Group IV with a one-way analysis level of significance $***p < 0.0001$ (Tukey's test). Further, (Tukey test) recellularized Group V ($n = 5$) showed an increase in DNA ng/ml and infected Group VA ($n = 5$) showed a decrease in DNA ng/ml in comparison to the Group V ($***p < 0.0001$)

elongated one. The renal cell expansion was reduced after achieving a 4–5 sub-culture. Vero cell line showed consistent expansion without any alteration even after regular passages (Fig. 4C).

3.5 Virus infection testing and culture

Intense positive reacted nsp-1 CHIKV serum was used for virus isolation and culture in Vero cells. nsp-1 negative serum was used as a negative control. Vero cells infected with CHIKV showed infectivity with the robust generation of CPE after 48 h. Vero cells exhibited CPE with virus release in cell suspension (Fig. 4D). The highest viral titre (serial fold) obtained was $1:10^{-1}$ to 10^{-7} on plaque assay.

3.6 Virus infection characterization

Immunofluorescence (IFA) was performed to detect CHIKV antigen in Vero cells (Fig. 4F). Negative control did not show any immunofluorescence (IFA) for CHIKV antigen (Fig. 4E).

3.7 Renal cell infectivity and viral titres

Culture (Group IIIA) renal cells were infected with CHIKV (0.01 MOI), and CPE was observed by 48 h (Fig. 4B). Later, released virion suspension was utilized for plaque assay. The viral titres on Vero cells for renal cells infection soup were transformed to $\text{Mean}_{\text{Log}} 10$ (Fig. 5) $5.925 \text{ pfu/ml} \pm 0.054$ (range 10^{-1} to 10^{-4} pfu/mL) (Fig. 5A, B). From this, it is absolute that even cultured renal cells can get infected with CHIKV.

3.8 Re-cellularization of kidney scaffold, CHIKV infection, histology, and plaque assays

Renal and Vero cells were perfused continuously into kidney scaffolds to be remodelled as per nephrological glomeruli network (Group V), which transformed kidney scaffold into viable re-cellularized graft (Fig. 6). Further, CHIKV infections were made to Group IA, IIA, VA. Group I, Group II, Group V showed no pathology (Fig. 6A–C). Group IIA did not show any pathological impairment due to CHIKV infection due to the absence of cells. The virus has lost its infectivity (Fig. 6E) at 37°C temperature. There was evident impairment observed in Group VA, where CHIKV showed its infectivity and replication (Fig. 6F). We performed plaque assays to assess viral infectivity in cultured and re-cellularized kidney scaffolds (Fig. 5A, B) (Table 1). Transformed mean \log_{10} viral titre (pfu/ml) difference between Group VA and Group IA was 0.322 pfu/ml, while Group IVA and Group IIIA was 0.36 pfu/ml. Group III and Group IV (control) suspension showed the absence of viral plaques (Fig. 5A).

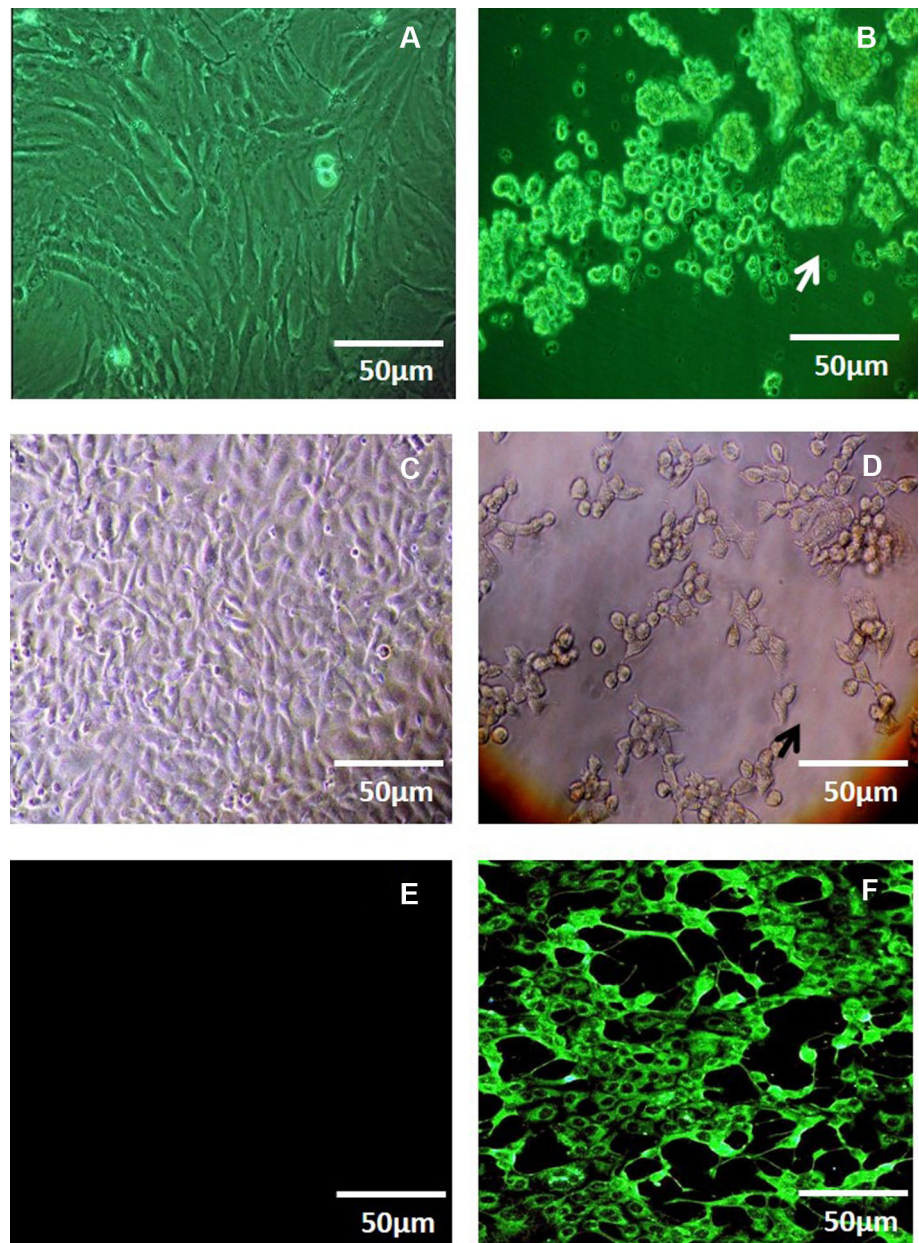
3.9 Plaques morphology

Group II showed complete decellularization with intact renal cortex, medulla, and vasculature (Fig. 1C, D). Group IA and Group VA non-perfused 1% crystal violet showed nodular cyst-like generation in the entire kidney area (Fig. 1E, G). Group IA and Group VA with perfused 1% crystal violet showed precise plaque formation with stained tissue zone in the background (Fig. 1F, H).

3.10 Malondialdehyde

MDA levels between infected and non-infected groups were quantified. The difference was observed in direct parallel relation (Fig. 7) (Table 1). Difference between Group IA and Group I showed 21.1 MDA nmoles/ml/mg protein, Group IIIA and Group III showed 19.86 MDA nmoles/ml/mg protein, Group IVA and Group IV 10.9 MDA nmoles/ml/mg protein, Group VA and Group V

Fig. 4 Renal cell and Vero cell culture and CHIKV infection characterization. **A** Confluent renal cells show spindle-like expansion in the culture. **B** Renal cells infected with CHIKV (48 h) with CPE generation. **C** Vero cells attain the confluence in culture after 24 h. **D** CHIKV infection to the Vero cells in culture with CPE generation and cell lysis after 48 h. **E** Negative staining for the anti-CHIKV marker. **F** Anti-CHIKV positive immunostaining with fluorescence signal



20.86 MDA nmoles/ml/mg protein. Thus, it indicates a rise in MDA levels in CHIKV-infected groups.

3.11 MTT assays

Results showed higher cell viability for non-infected groups and lesser cell non-viability (Fig. 8) (Table 1). It was interesting to note that CHIKV infection showed lesser cell viability and higher non-viability, indicating virus propagation within cellular systems.

4 Discussion

Chikungunya, a globally affecting disease, leads to crippling arthralgia and myalgia which lasts for years and poses essential public health threat [8–12]. It targets the brain, cartilage, joints, bones and triggers bone loss by increasing RANKL/OPG ratio [13–15]. Several chemokines have been associated with chemotaxis (CXC) of osteoclast cell precursors and osteoclastogenesis in pathological bone conditions, including multiple myeloma [16]. CHIKV is traditionally propagated in various cell culture models and animal models [17]. However, both methods have certain limitations. Vero cell cultures for CHIKV

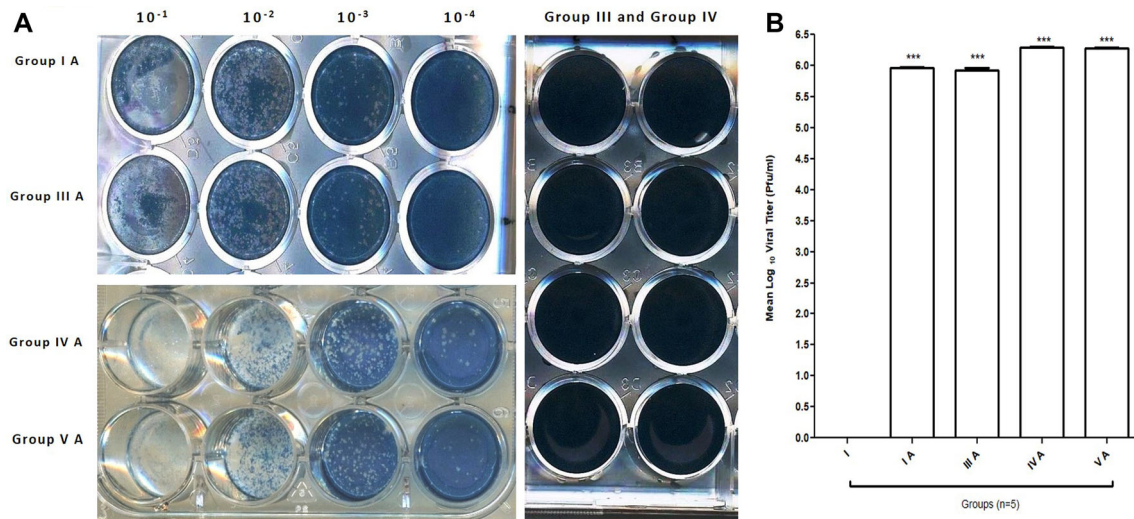


Fig. 5 **A** Plaques quantification and analysis for the infected and non-infected groups. The Group IV-A and Group VA showed a rise in viral titre compared to all other groups with one-way analysis of variance (Tukey's test) $***p < 0.0001$. Plaque generation and viral titre were completely absent for Group III ($n = 5$) and Group IV ($n = 5$) showing a one-way ANOVA $***p < 0.0001$ level of

significance. However, Group IA and Group IIIA showed a reduction in plaques and viral titre than Group IV A and Group VA with a one-way analysis level of significance $***p < 0.0001$ (Tukey's test). **B** The transformed Mean log₁₀ viral titre were also similar to plaque assays (One-way analysis of variance)

expansion will provide CPE generation but fails to offer the exact role of the virus in ECM alteration. Vaccine prepared in chick embryo suspension cultures was significantly more protective than those prepared in a monolayer of kidney cells in mice models [18]. Expanded CHIKV in mice's brains for developing antibodies has also shown limitation as treatment modality [19]. Likewise, the use of animal models poses certain ethical issues and possibility of contaminations cannot be ruled out. Hence, there is a need for alternative method which can provide abundant and cost-effective viral expansion that can be utilised to study their life cycles, to prepare vaccines or anti-pathogen drugs, and many more.

A fully functional tissue-engineered kidney was fabricated by perfusion technology for kidney transplantation [6, 7] and to study nephrological vasculature network before [20]. For the first time, we used this bio-model to act as a natural niche for CHIKV. Its propagation in the T-E kidney is compared with that in the control kidney and cell culture using renal and Vero cell lines. Our findings allow us to study the replication of CHIKV and pathological alteration in ECM. We observed that after infection, CHIKV didn't replicate in the scaffold due to the absence of cells. The plaque generation was higher in Group IA compared to Group VA (Fig. 1D, E and H). Group I had normal nephrological architecture, including cells and ECM, whereas, Group II had intact ECM without any cells (Fig. 6A, B). Group IA and VA showed impaired cells and distorted ECM (Fig. 6D, F). Group IIA exhibited no

pathological effect due to a lack of viral sustainability (Fig. 6E).

The critical part of scaffold fabrication is to check the occurrence of host residual ds-DNA. Group, I showed the maximum occurrence of ds-DNA in comparison to Group IA. Group II exhibited minimal levels of ds-DNA due to the absence of cells. Group III showed more deficient ds-DNA levels compared to Group IV. Group V showed an enhanced ds-DNA level compared to Group III and IV, indicating renal and vero cell propagation (DNA-replicates) within the kidney scaffold. The ds-DNA levels were decreased for all groups infected with CHIKV (Fig. 3).

Plaque assays show transformed mean log₁₀ viral titre for CHIKV-infected groups. Non-infected Groups III and IV did not show any viral titre (Fig. 5A). Plaque formed in culture (Fig. 4B, D) and in the T-E kidney (Fig. 5A) showed that CHIKV could infect and replicate various model groups. The viral titre of Group VA was nearer to that of Group IVA than other CHIKV-infected groups (Fig. 5B). To observe gross morphological pathology developed in kidney and re-cellularized kidney scaffolds, we had perfused 1% crystal violet dye in Group IA and Group VA. CHIKV formed plaques within kidney showed translucent whitish zones for Group IA and Group VA, indicating infection developed in the capsule (Fig. 1H).

Malondialdehyde is a hallmark (biomarker) of imbalances of redox reactions progressing transmembrane domain fatty acid peroxidation, DNA (oxidation) fragmentation, and cell apoptosis [20, 21]. We investigated lipid peroxidation (inflammatory) levels for non-infected

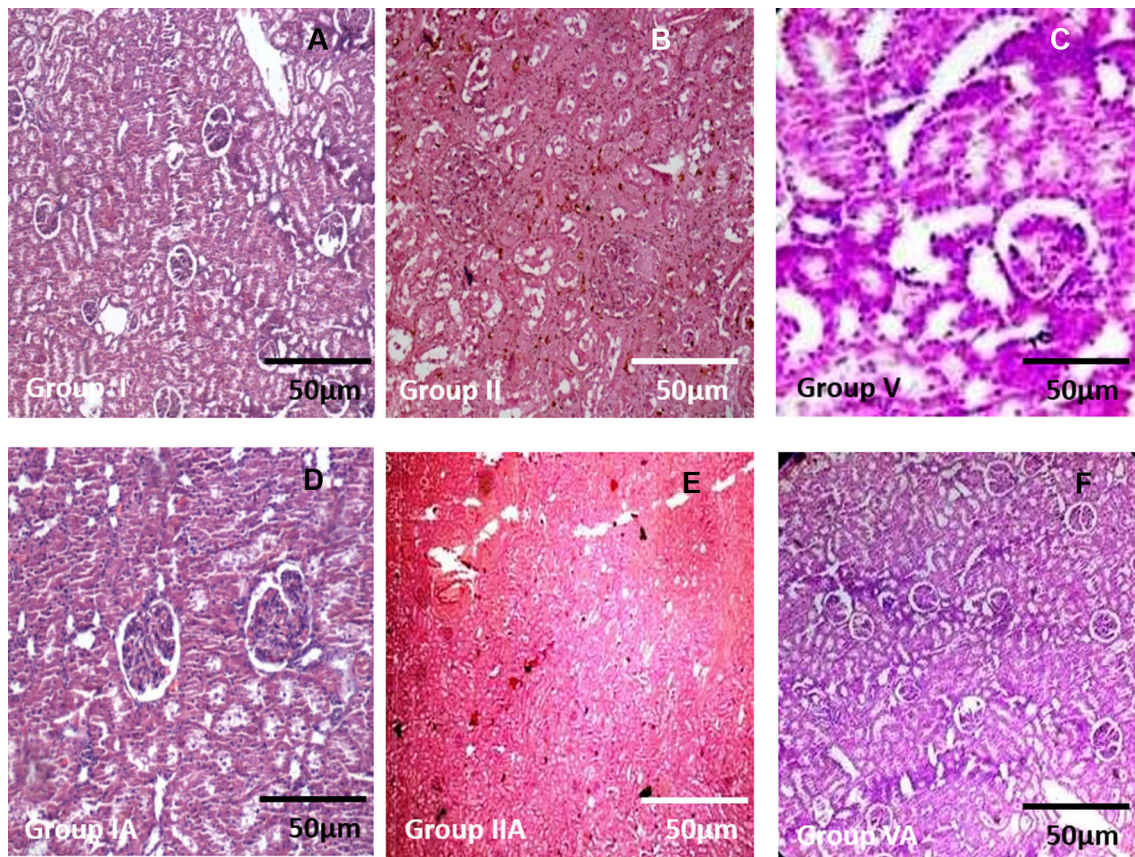


Fig. 6 **A** Histology (Hematoxylin and Eosin staining) for non-infected Group I showed intact cellular organization of cuboidal cells along with PCT and DCT phenotype. **B** Group II showed a complete absence of cells along with decellularization. **C** Group V showed the re-cellularization of kidney scaffolds towards the remodeling of the renal and Vero cells. **D** The CHIKV infection to the kidney (Group

IA) showed a cytopathological effect in the glomerulus network with the impaired matrix. **E** There was no impairment observed in the Group IIA scaffolds. **F** The Group VA showed a similar type of cytopathological infection development in the cells and alteration in the ECM

and infected groups (Fig. 7). MDA levels in Group I was higher than Group III, IV, and V due to intact tissue. There was not much difference in MDA observed between Group III and IV. In contrast, Group V levels were higher than Group III and II but lesser than Group I. CHIKV-infected groups (Fig. 7) significantly enhanced MDA levels in non-infected groups due to cellular inflammation-causing excess peroxidation. Peroxidation and DNA replication had a direct role in metabolic activity and cell division [22]. Cellular proliferation (MTT) and viability were studied which showed formazan crystal generation during cellular activity and expansion quantified as viability [23]. The inversely proportional graph that was plotted was non-viability (Fig. 8). CHIKV-infected groups showed higher percentage of non-viability as compared to non-infected groups. Most escalated cell viability activity was found in Group I, whereas the highest non-viability was found for Group VA. There was a consistent rise in cell viability and constant downfall in non-viability for non-infected groups such as Group III, Group IV, and Group V. CHIKV

infected groups showed stepwise consistency rise for non-viability (Group IA, Group IIIA, Group IVA, and Group VA) (Fig. 8).

Overall, the T–E kidney gave us excellent and economical media for abundant CHIKV propagation. The method also allowed us to investigate role of CHIKV in developing renal pathology along with alteration in cells and ECM. Understanding incentives that promote and maintain CHIKV and a plethora of dynamics is essential to combat the virus's emergence and spread. Although the mortality rate of CHIKV disease is modest, the morbid and chronic nature of CHIKV disease and its associated economic burden are essential considerations for developing specific treatments. An ideal vaccine should induce a potent immune response with a single dose at a low cost. Our study throws light on a novel methodology for virus propagation and fabricated system to study their direct pathological effect on live re-engineered organs and test antiviral drugs' efficacy on viral titres.

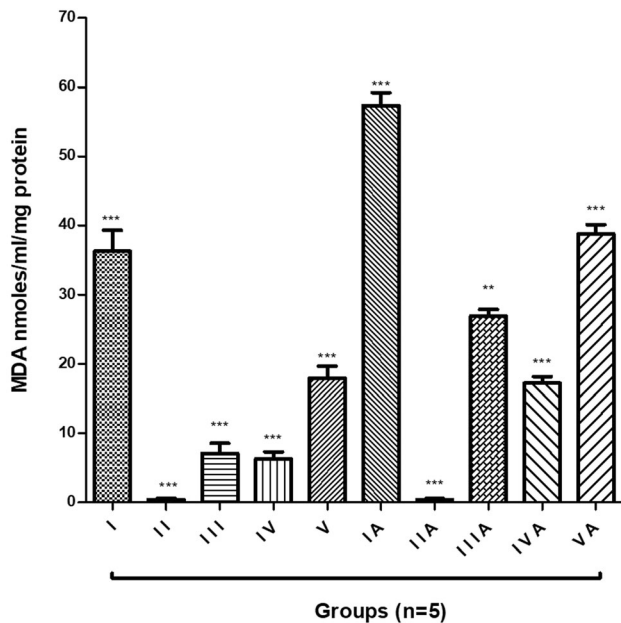


Fig. 7 Lipid peroxidation (MDA nmol/ml/mg protein) for Group I, Group II, Group III, Group IV, Group V, Group IA, Group II-A, Group III-A, Group IV A and Group V A was estimated and the level of significance $*p < 0.0001$ (One-way ANOVA) was calculated. The comparison was also made between non-infected groups and CHIKV-infected groups (Tukey's test). The non-infected Groups I, II, III and IV showed lesser MDA nmoles/ml/mg proteins. In comparison to CHIKV-infected groups such as Group IA, Group II-A, Group III-A, Group IV A, and Group V A. If compared MDA levels between non-infected groups, it was observed that Group I has higher levels of MDA levels than cell culture (Group III and Group IV) and re-cultured (Group V) groups. The CHIKV-infected groups showed enhanced MDA levels than non-infected groups

Although recent studies have contributed to a better understanding of the basic biology of CHIKV replication and disease, future work on virus-vector interactions, molecular mechanisms of viral replication, careful deconstruction of multifaceted CHIKV-induced immune responses, pathological destruction of target organs and other systems, and development of therapeutic interventions will be required to combat CHIKV transmission and illness. A cost-effective, ethically approved, fast-track, abundant source of virus is essential for future studies and in pharmaceuticals. The unique technique of using tissue-engineered bio-model to study virulent and non-virulent pathogens is only answer, and it will open new gates for virologists, clinicians. Current work will be of particular interest to the biomedical industry, which is involved in developing innovative clinical therapeutic approaches in antiviral drug testing or vaccine design.

Acknowledgements SW and SA designed the study. SW and SA carried all the experiments. SA analyzed all the results data. SW and SA interpreted the results and wrote the manuscript. SA advised on

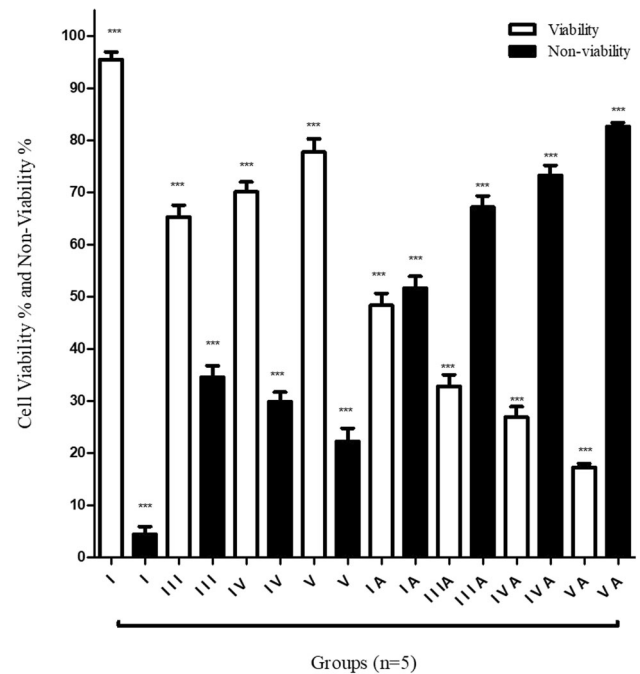


Fig. 8 The MTT assays showed cell viability higher towards the non-infected groups and lesser non-viability. The CHIKV-infected groups showed higher non-viability and lesser cell viability. The level of significance ($***p < 0.0001$) was obtained for cell viability and non-viability through One-way analysis of variance (Tukey test)

manuscript content and communications. All authors approved the submission of the final version of the manuscript to be published.

Declarations

Conflict of interest The author(s) declared no potential competing/conflicts of interest for the research, authorship, and publication of this article.

Ethical statement All protocols were approved by HEALTH BIO-LABS, Shree Hospital & Research Institute Ethics Committee (HBL-SHREC), Kolhapur, India.

References

1. Taubitz W, Cramer JP, Kapaun A, Pfeffer M, Drosten C, Doblér G, et al. Chikungunya fever in travelers: clinical presentation and course. *Clin Infect Dis*. 2007;45:e1-4.
2. Hochedez P, Jaureguierry S, Debruyne M, Bossi P, Hausfater P, Brucker G, et al. Chikungunya infection in travellers. *Emerg Infect Dis*. 2006;12:1565–7.
3. Powers AM, Logue CH. Changing patterns of Chikungunya virus: re-emergence of a zoonotic arbovirus. *J Gen Virol*. 2007;88:2363–77.
4. Kirchhausen T, Owen D, Harrison SC. Molecular structure, function, and dynamics of clathrin-mediated membrane traffic. *Cold Spring Harb Perspect Biol*. 2014;6:a016725.
5. Paredes AM, Ferreira D, Horton M, Saad A, Tsuruta H, Johnston R, et al. Conformational changes in sindbis virions resulting from exposure to low pH and interactions with cells suggest that cell

- penetration may occur at the cell surface in the absence of membrane fusion. *Virology*. 2004;324:373–86.
6. Song JJ, Guyette JP, Gilpin SE, Gonzalez G, Vacanti JP, Ott HC, et al. Regeneration and experimental orthotopic transplantation of a bioengineered kidney. *Nat Med*. 2013;19:646–51.
 7. Sullivan DC, Mirmalek-Sani SH, Deegan DB, Baptista PM, Aboushwareb T, Atala A, et al. Decellularization methods of porcine kidneys for whole organ engineering using a high-throughput system. *Biomaterials*. 2012;33:7756–64.
 8. Mishra P, Kumar A, Mamidi P, Kumar S, Basantray I, Saswat T, et al. Inhibition of Chikungunya virus replication by 1-[(2-methylbenzimidazol-1-yl) methyl]-2-oxo-indolin-3-ylidene] amino] thiourea (MBZM-N-IBT). *Sci Rep*. 2016;6:20122.
 9. Almelkar SI, Bethapudi S, Rath SN. Development of an experimental model of a decellularized kidney scaffold by perfusion mode and analyzing the three-dimensional extracellular matrix architecture by edge detection method. *Indian J Nephrol*. 2018;28:339–44.
 10. Pialoux G, Gaüzère BA, Jauréguiberry S, Strobel M. Chikungunya, an epidemic arbovirolosis. *Lancet Infect Dis*. 2007;7:319–27.
 11. Pavri KM. Presence of the Chikungunya antibodies in human sera collected from Calcutta and Jamshedpur before 1963. *Indian J Med Res*. 1964;52:698–702.
 12. Lim EXY, Supramaniam A, Lui H, Coles P, Lee WS, Liu X, et al. Pathogenesis as a source of virus replication and soluble factor production. *Viruses*. 2018;10:86.
 13. Rulli NE, Melton J, Wilmes A, Ewart G, Mahalingam S. The molecular and cellular aspects of arthritis due to alphavirus infections: lesson learned from Ross River virus. *Ann N Y Acad Sci*. 2007;1102:96–108.
 14. Lim PJ, Chu JJ. A polarized cell model for Chikungunya virus infection: entry and egress of virus occurs at the apical domain of polarized cells. *PLoS Negl Trop Dis*. 2014;8:e2661.
 15. Noret M, Herrero L, Rulli N, Rolph M, Smith PN, Li RW, et al. Interleukin 6, RANKL, and osteoprotegerin expression by Chikungunya virus-infected human osteoblasts. *J Infect Dis*. 2021;206:455–9.
 16. Chen W, Foo SS, Taylor A, Lulla A, Merits A, Hueston L, et al. Bindarit, an inhibitor of monocyte chemotactic protein synthesis, protects against bone loss induced by Chikungunya virus infection. *J Virol*. 2015;89:581–93.
 17. Myers RM, Carey DE, Reuben R, Jesudass ES, De Ranitz C, Jadhav M. The 1964 epidemic of dengue-like fever in South India: isolation of Chikungunya virus from human sera and from mosquitoes. *Indian J Med Res*. 1965;53:694–701.
 18. White A, Berman S, Lowenthal JP. Comparative immunogenicities of Chikungunya vaccines propagated in monkey kidney monolayers and chick embryo suspension cultures. *Appl Microbiol*. 1972;23:951–2.
 19. Rampal SM, Meena H. Neurological complications in Chikungunya fever. *J Assoc Phys India*. 2007;55:765–9.
 20. Almelkar SI, Divate S, Patwardhan AM. Bacopa monniera herb as an antioxidant in reducing lipid peroxidation levels in cultured human endothelial cells. *J Cell Tissue Res*. 2013;13:3549–56.
 21. Walawalkar S, Almelkar S. Fabricating a pre-vascularized large-sized metabolically-supportive scaffold using Brassica oleracea leaf. *J Biomater Appl*. 2021;36:165–78.
 22. Walawalkar S, Verma MK, Almelkar S. Re-endothelization of human saphenous vein scaffold surfaces for bioprosthesis fabrication. *J Biomater Appl*. 2020;34:1081–91.
 23. Walawalkar S, Almelkar S. Fabrication of aortic bioprosthesis by decellularization, fibrin glue coating, and re-endothelization: a cell scaffold approach. *Prog Biomater*. 2019;8:197–210.

Publisher's Note Springer Nature remains neutral with regard to jurisdictional claims in published maps and institutional affiliations.